Macromolecular Rapid Communications
www.mrc-journal.de

Cell Adhesion on UV-Crosslinked Polyurethane Gels with Adjustable Mechanical Strength and Thermoresponsiveness

*Katharina Breul, Elena Stengelin, Moritz Urschbach, Mihail Mondeshki, Laura Wüst, Jason Sirleaf, Sebastian Seitel, Theresa Emt, Sarah Pschierer, Pol Besenius, and Sebastian Seiffert**

Temperature-responsive polyurethane (PU) hydrogels represent a versatile material platform for modern tissue engineering and biomedical applications. However, besides intrinsic advantages such as high mechanical strength and a hydrolysable backbone composition, plain PU materials are generally lacking bio-adhesive properties. To overcome this shortcoming, the authors focus on the synthesis of thermoresponsive PU hydrogels with variable mechanical and cell adhesive properties obtained from linear precursor PUs based on poly(ethylene glycol)s (pEG) with different molar masses, isophorone diisocyanate, and a dimerizable dimethylmaleimide (DMMI)-diol. The cloud point temperatures of the dilute, aqueous PU solutions depend linearly on the amphiphilic balance. Rheological gelation experiments under UV-irradiation reveal the dependence of the gelation time on photosensitizer concentration and light intensity, while the finally obtained gel strength is determined by the polymer concentration and spacing of the crosslinks. The swelling ratios of these soft hydrogels show significant changes between 5 and 40 °C whereby the extent of this switch increases with the hydrophobicity of the precursor. Moreover, it is shown that the incorporation of a low amount of catechol groups into the networks through the DMMI dimerization reaction leads to strongly improved cell adhesive properties without significantly weakening the gels.

1. Introduction

Thermoresponsive hydrogels are one of the most promising material platforms for modern biomedical applications with a scope ranging from nanomedical drug carriers to 3D in vitro models and tissue engineering applications.[1,2] Especially in the latter cases, it is crucial to provide soft materials which resemble the biological extracellular matrix. To ensure an efficient nutrient and waste transport as well as tissue-like mechanical properties, this requires hydrogels with swelling ratios between 50–85 wt%.[3,4] Depending on the respective application, the adaptive hydrogels should further be cell adhesive, biodegradable, and exhibit robust and distinct thermoresponsive properties.

While natural hydrogels such as protein gels usually fulfill the bio-related requirements, their weak mechanical properties as well as the batch-to-batch variations resulting from their animal-based origins limit the application scope.[5,6] In contrast, the chemical and mechanical properties of synthetic hydrogels are by far easier to adjust to the application specific demands. However, synthetic materials are usually bioinert, and cell-adhesion must be enabled through additional bio-linkers or coatings that allow interactions with cell surface receptors.[7–10] Due to these complementary properties, the development of hydrogel platforms that combine the advantages of natural and synthetic materials is an ongoing challenge for materials scientists.

Regarding the thermal adaptivity of responsive hydrogels, poly(*N*-isopropylacrylamide) (pNiPAm) is still the most common polymer backbone due to its sharp volume phase transition (VPT) close to the physiological temperature range in aqueous media. Nevertheless, it has drawbacks. Although much progress was achieved with respect to the often insufficient mechanical performance of pNiPAm-based hydrogels,[11] fundamental issues such as the non-degradability of the vinyl backbone remain.[12] To provide versatile alternatives, thermoresponsive polyurethane (PU) hydrogels received increasing interest. The general biocompatibility of PU materials is widely established and enabled various medical applications ranging from controlled drug delivery carriers[13–15] to promising or already commercialized materials for blood contacting devices like prosthetic heart valves.[16] In these materials, the urethane groups in the polymer backbone are

K. Breul, E. Stengelin, M. Urschbach, M. Mondeshki, L. Wüst, J. Sirleaf, S. Seitel, T. Emt, S. Pschierer, P. Besenius, S. Seiffert
Department of Chemistry
Johannes Gutenberg-University Mainz
Duesbergweg 10–14, Mainz 55128, Germany
E-mail: sebastian.seiffert@uni-mainz.de

The ORCID identification number(s) for the author(s) of this article can be found under https://doi.org/10.1002/marc.202100505

DOI: 10.1002/marc.202100505

not only responsible for the often superior mechanical strength of PU networks but are also intrinsically hydrolysable.[14,17–19]

To obtain thermoresponsive PUs, the combination of a hydrophilic oligomeric diol (soft segment) and a hydrophobic diisocyanate (hard segment) has been established as versatile design approach. Due to its commercial availability, pronounced hydrophilicity and nontoxicity, poly(ethylene glycol) (pEG) became the most commonly applied soft segment. As shown by Fu et al., the variation of the polyether molar mass and thus the molar ratio of hydrophilic and hydrophobic segments allows for an easy variation of the lower critical solution temperature (LCST) of such amphiphilic PUs in aqueous solution.[18] Nevertheless, it should be noted that their turbidity measurements showed a rather broad (≈10 °C) and partially incomplete LCST transition in comparison to pNiPAm. This has been strongly improved through the introduction of charged comonomers, which further allowed an even more flexible variation of the LCST, as demonstrated by Sardon et al.[13,20]

To transfer the obtained insights from linear chains to 3D crosslinked networks, PU hydrogels have either been obtained in a crosslinking polymerization in the presence of a trifunctional comonomer[17,21,22] or through the consecutive crosslinking of linear precursor polymers with reactive side-groups.[20,23] As shown in the studies of Frydrych et al. and Li et al., the absolute swelling ratio of such PU gels can be variated through the molar mass of the polyether soft segment in both cases. The comparison of the equilibrium swelling ratios Q (in wt%) at 4 and 40 °C demonstrates a $Q_{4\,°C}/Q_{40\,°C}$ switching of ≈100% in a purely pEG based system[17] while up to 600% can be achieved through the implementation of oligo(ethylene glycol) side chains as demonstrated by Aoki and Ajiro.[22]

Despite the numerous improvements achieved with respect to the processability, mechanical performance, and thermal adaptivity of pEG-based PU hydrogels, strategies to achieve cell adhesion have been rarely implemented. To overcome this limitation, in the present work, we apply the modular design principles established for thermoresponsive PUs to create hydrogels with adjustable mechanical strength and thermoresponsiveness that can additionally be bio-activated through the covalent attachment of cell-adhesive groups. As a consecutive crosslinking strategy provides a greater flexibility with respect to the material's processability, we focus on the synthesis of linear PUs based on pEG and isophorone diisocyanate (IPDI). To avoid unspecific crosslinking, toxic catalysts or a strong pH dependency, an uncharged dimethylmaleimide (DMMI) comonomer is incorporated as a reactive side-group which undergoes a dimerization reaction in the presence of a photosensitizer and UV light.[24] To improve the cell adhesion on these gels, we further attach arginine-glycine-aspartate- (RGD) amino acid sequences and catechol groups to the network through the identical DMMI dimerization reaction.

2. Results and Discussion

2.1. Thermoresponsive, UV-Crosslinkable Polyurethanes

Linear PUs are synthesized in a prepolymer procedure starting from pEG diols with differing molar masses (M_n ≈ 1.0 (**1a**), 1.5 (**1b**), 2.0 (**1c**), and 4.0 (**1d**) kg•mol^{-1}) that are added to the asymmetric isophorone diisocyanate (IPDI) **2** and converted into the corresponding macrodiisocyanates (pEG/IPDI) **3a–d** by reaction with the cycloaliphatic, secondary isocyanate group under organo-tin catalysis (**Figure 1**A).[25–27] To incorporate dimerizable DMMI-groups, 2,3-dimethyl maleic anhydride **10** is first attached to a hydrophilic triethylene glycol linker **9**, which is coupled with the acetonide protected 2,2-bis(hydroxymethyl)propionic acid **14** as shown in Scheme S1, Supporting Information. The deblocked DMMI-diol **4** is then applied as chain extender for the pEG diisocyanates **3a–d**. Size exclusion chromatography (SEC) measurements of the pEG diols **3a–d** and the obtained linear PUs **5a–e** demonstrate moderately effective but sufficient chain elongation efficiencies as summarized in **Table 1** and Figure S2, Supporting Information.

The molar ratios between the hydrophilic ethylene glycol (EG) units of the pEG backbone and the hydrophobic IPDI-DMMI blocks are investigated by ^{1}H-NMR spectroscopy. Comparing the characteristic signals of the DMMI methyl groups (1.89 ppm), the IPDI cycloaliphatic methylene- and methyl-groups (1.19–0.06 ppm) and the pEG backbone (3.76–3.40 ppm) reveals the intended increase of the molar content of hydrophilic EG groups with the molar mass of the polyether (Table 1 and Figures S20–S24, Supporting Information). To enable an even finer variation of the hydrophilic-to-hydrophobic balance than accessible through the commercially available pEG diols, the molar feed ratio between pEG and DMMI is additionally varied from 1:1 to 1:2.3 for pEG-1.5k (PU-1.5k$^{0.6}$ **5b**). The ^{1}H-NMR analysis verifies that this approach is another facile option to alter the PU composition. All experimental details and full characterizations can be found in the Supporting Information.

To investigate how the variation of the amphiphilic balance influences the thermoresponsivity, the cloud point temperatures T_{CP} are determined through UV–Vis transmittance measurements in dilute aqueous solutions (**Figure** 1B). As shown in Figure 1C, the cloud point temperatures depend linearly on the molar ratio between hydrophilic EG and hydrophobic IPDI and DMMI groups and can be varied from 5 to over 90 °C. In accordance with the observations reported by Li et al. and Ronco et al., the turbidity curves depicted in **Figure 2**B also reveal a sharper and more pronounced LCST transition for the more hydrophobic PU compositions.[20,23]

2.2. Gelation and Mechanical Properties

Further on, the UV-induced crosslinking of the linear precursor polymer solutions in the presence of the photosensitizer thioxanthone disulfonate (TXS) is investigated by linear shear rheological experiments. Applying PU-4.0k **5e** (c_{PU} = 100 g•L^{-1}) as a representative example, the gelation time in terms of the G'–G'' crossover is determined as t_{gel} = 8 min at a TXS concentration of 1 mM and an irradiation aperture of 1%, and is shown to be temperature independent between 5–20 °C (Figure S3, Supporting Information). When the TXS concentration is reduced to 0.1 mM while the irradiation intensity is kept constant at 1%, the gelation time increases to 68 min while the obtained gel strength remains constant. The gelation time at the lower TXS concentration (0.1 mM) can however be reduced to 7 min if the irradiation aperture is increased to 10%. This qualitative parameter screening demonstrates how the gelation time of the DMMI crosslinked

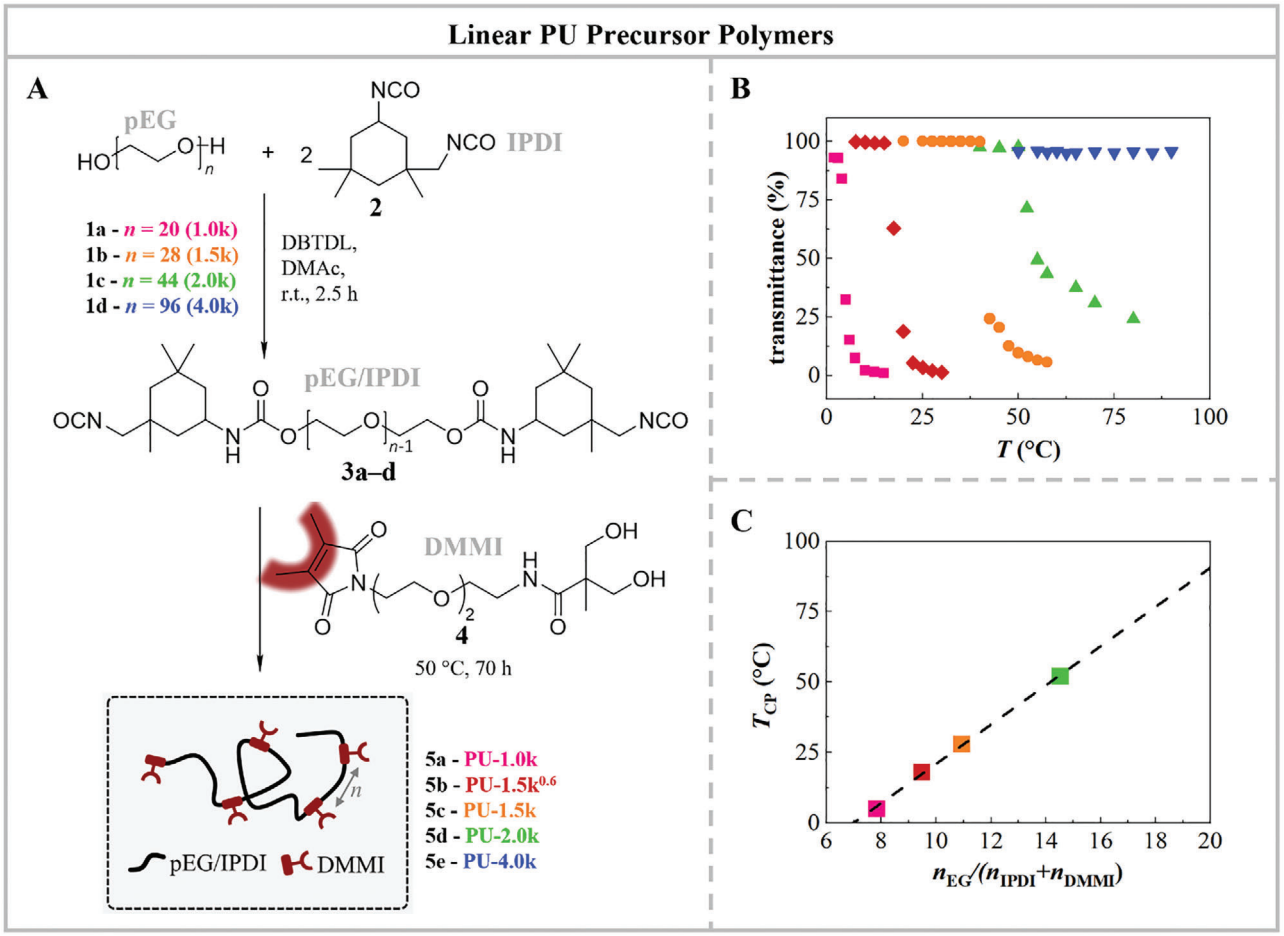

Figure 1. A) Synthesis of linear pEG/IPDI-based PUs with DMMI pendant groups (**5a–e**). B) Turbidity measurements of PU-1.0k **5a** (■, pink), PU-1.5k$^{0.6}$ **5b** (◆, red), PU-1.5k **5c** (●, orange), PU-2.0k **5d** (▲, green), and PU-4.0k **5e** (▼, blue) in water (5 g•L^{-1}). C) Cloud point temperatures as a function of the molar ratio between EG, IPDI, and DMMI with linear regression (dashed line).

Table 1. pEG diols applied in the polymerization. Characterization of the synthesized PUs.

#	M_n (pEG diol) [kg mol^{-1}]$^{a)}$	M_w [kg mol^{-1}]$^{a)}$	$Đ^{a)}$	$n_{EG}/n_{IPDI}/n_{DMMI}$ $^{b)}$	T_{cp} [°C]
5a – PU-1.0k	0.88	6.3	1.5	29:2.7:1	5
5b – PU-1.5k$^{0.6}$	1.24	12.0	1.9	36:2.8:1	18
5c – PU-1.5k	1.24	12.4	1.8	47:3.3:1	28
5d – PU-2.0k	1.95	14.6	1.6	61:3.2:1	52
5e – PU-4.0k	4.22	30.3	1.5	140:4.5:1	>90

$^{a)}$ SEC (DMF, pEG calibration) $^{b)}$ ^{1}H-NMR analysis (EG: 3.76–3.40 ppm, 4H; IPDI: 1.19–0.06 ppm, 15H; DMMI: 1.89 ppm, 6H)

hydrogels can be readily adjusted by these two external parameters.

Next, we investigate how the gel strength in terms of the plateau modulus depends on the precursor polymer concentration of PU-4.0k **5e** (T = 5 °C). As indicated in **Figure** 2A, no stable gel is obtained below a concentration of c_{PU} = 100 g•L^{-1}. Above this gelation threshold, the plateau moduli increase approximately linearly from 200 to 3900 Pa with the polymer concentration (Figure 2B), as expected for affine and phantom networks. It should be noted though, that the precursor solutions then become increasingly viscous (Figure 2A) which leads to inhomogeneities and handling difficulties.

Further on, we compare the mechanical properties of hydrogels obtained from the different precursor polymers (c_{PU} = 100 g•L^{-1}). PU-1.0k **5a** is excluded from all further experiments due to its incomplete dissolution in water at higher polymer contents. As shown in Figure 2C, the time-dependent plateau moduli clearly demonstrate the dependency of the gel strength on the average sticker spacing, which is mainly determined by the pEG molar mass (Figure 2D). As expected, the PU-1.5k$^{0.6}$ **5b** hydrogel

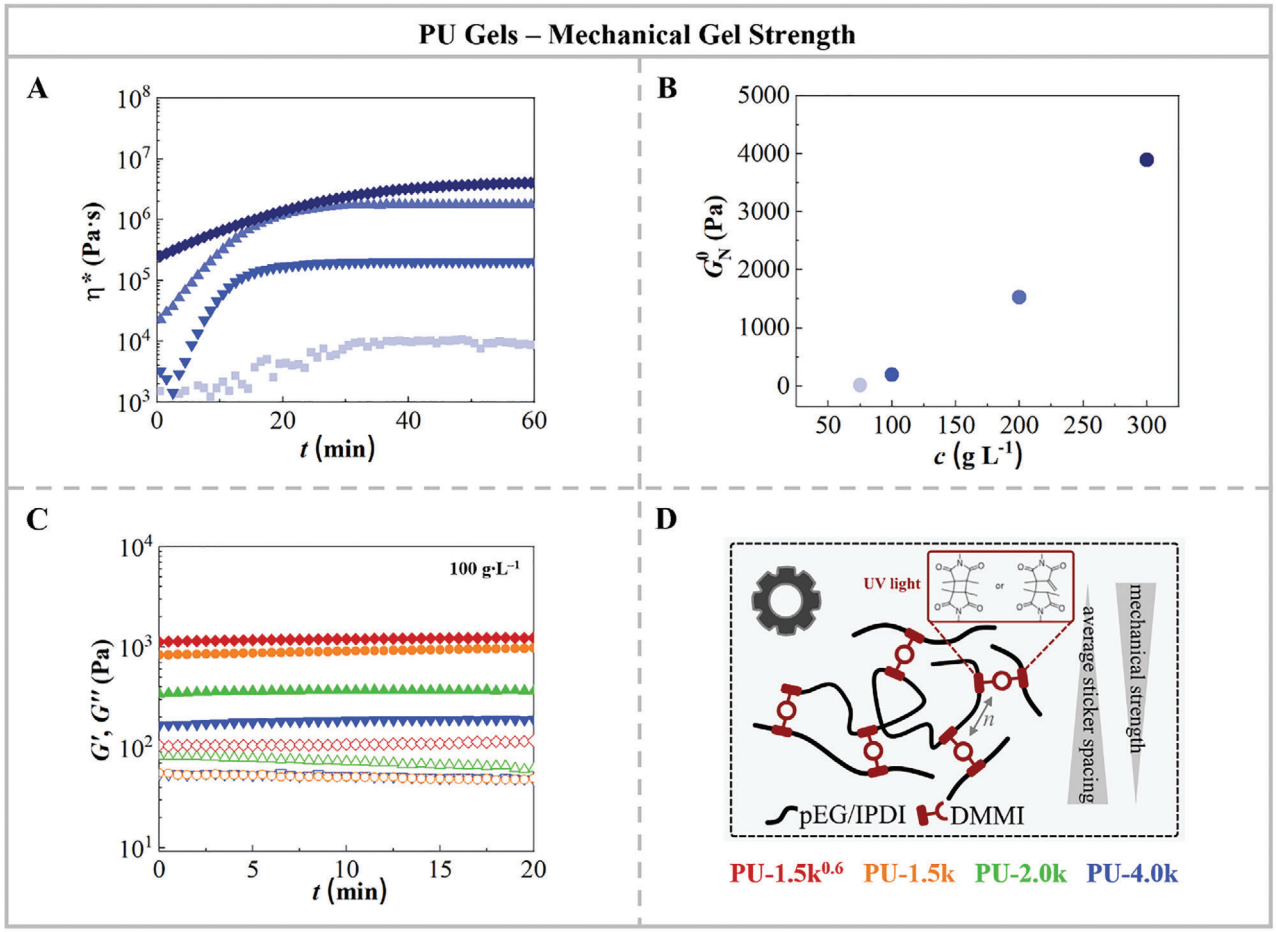

Figure 2. A) Time-dependent complex viscosity of PU-4.0k **5e** solutions under UV irradiation at a concentration of 75 (■), 100 (▼), 200 (▲), and 300 g•L^{-1} (◆). Gelation occurs at a TXS concentration of 1 mM, an irradiation aperture of 1% (320–500 nm), and at a temperature of 5 °C. B) Plateau moduli as a function of the PU-4k concentration (same color code as before). C) Time-dependent storage G' (closed symbols) and loss G'' moduli (open symbols) of PU-1.5k$^{0.6}$ **5b** (◆, red), PU-1.5k **5c** (●, orange), PU-2.0k **5d** (▲, green), and PU-4.0k **5e** (▼, blue) hydrogels at a concentration of 100 g•L^{-1} (T = 5 °C). D) Schematic representation of the DMMI crosslinked PU networks.

shows the highest plateau modulus (1200 Pa), which decreases with the pEG content and molar mass to 990 Pa (PU-1.5k **5c**), 370 Pa (PU-2.0k **5d**), and finally 200 Pa (PU-4.0k **5e**). In summary, the concentration and precursor polymer dependent mechanical properties are qualitatively consistent with the expected structure–property relations and allow an easy adjustment of the gel strength between 200–4000 Pa though the precursor polymer concentration and average sticker density.

2.3. Swelling Properties of PU Hydrogels

To investigate the temperature-dependent hydration behavior (**Figure 3**A), the swelling degrees of PU gels crosslinked at c_{PU} = 100 g•L^{-1} are measured at 5, 20, and 40 °C after equilibration for 12 h at each temperature. Note that the synthesized hydrogels are thoroughly dialyzed beforehand to avoid interferences with a potentially occurring sol fraction. It can first be observed that the swelling degrees of the fully hydrated networks at 5 °C show the same crosslinking-density dependency as the gel strength and increase from 2700% (PU-1.5k$^{0.6}$) over 4100% (PU-1.5k) and 5000% (PU-2.0k) to 7800% (PU-4.0k) with increasing soft segment length (Figure 3B). This tendency is in accordance with the findings reported by Li et al. and Frydrych et al. who also variated the pEG molar mass in chemically crosslinked PU hydrogels and investigated their temperature-dependent equilibrium swelling.[17,23]

The thermal responsiveness of the hydrogels is further evaluated by comparing the equilibrium swelling degrees at 5 and 40 °C. As depicted in Figure 3C, the temperature induced volume switch decreases around a factor two from (350 ± 12)% (PU-1.5k$^{0.6}$ **5b**) to (180 ± 4)% (PU-4.0k **5e**) from the most hydrophobic to the most hydrophilic PU composition. This trend qualitatively reflects the LCST behavior of the dilute precursor polymer solutions which was shown to depend linearly on the balance between hydrophilic EG and hydrophobic DMMI- and IPDI-monomers (Figure 1C). However, within the crosslinked gels this dependency is not as clearly pronounced and the volume switches of the PU-1.5k$^{0.6}$ and PU-1.5k gels even coincide within the margin of error. Note, that the considerable weighing error and small

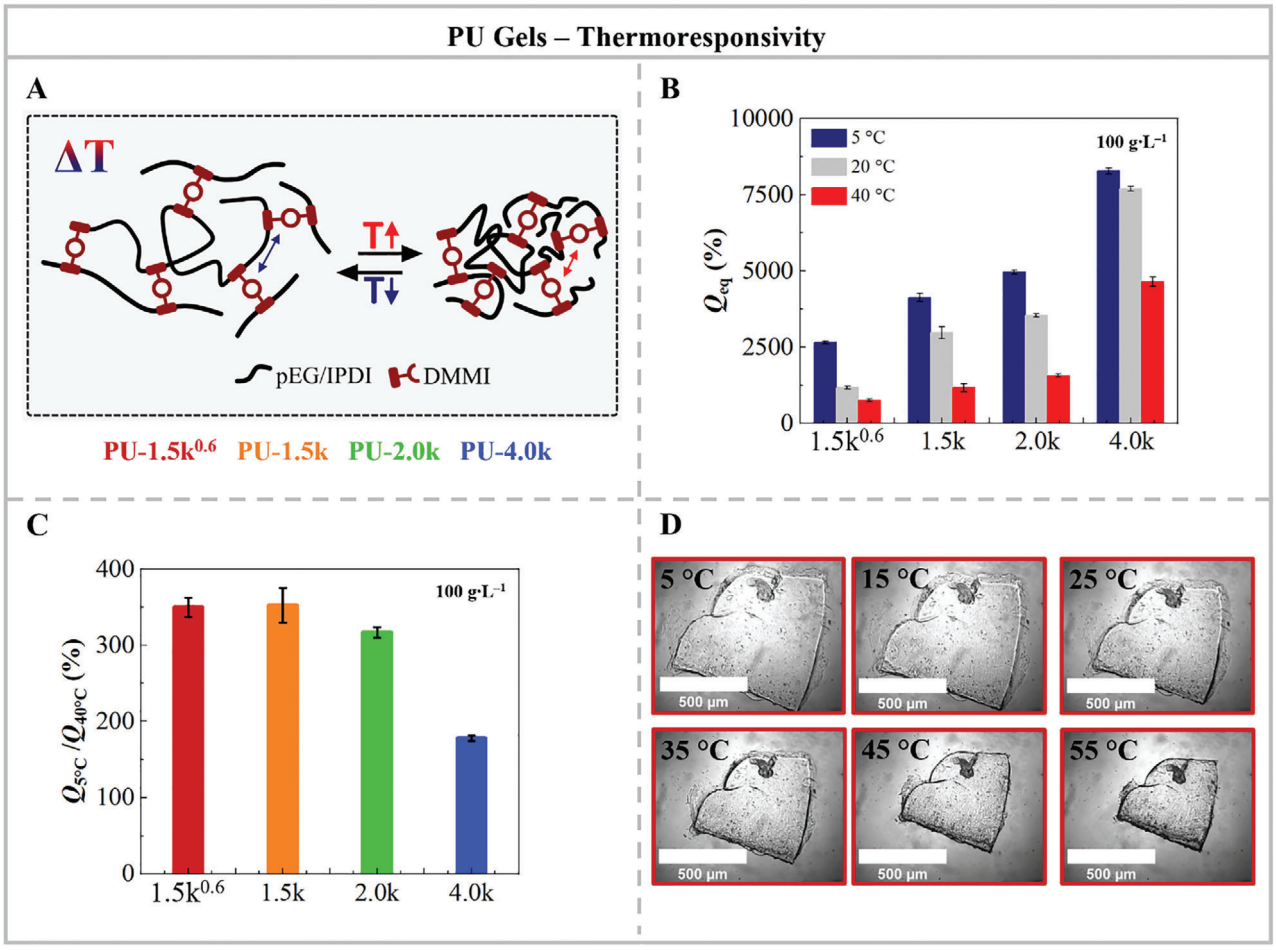

Figure 3. A) Schematic representation of the temperature-induced hydrogel deswelling. B) Equilibrium swelling degrees and C) swelling degree switches between 5 and 40 °C of PU-1.5k$^{0.6}$ **5b** (red), PU-1.5k **5c** (orange), PU-2.0k **5d** (green), and PU-4.0k **5e** (blue) hydrogels crosslinked at a concentration of 100 g•L^{-1} and equilibrated for 12 h at 5, 20, and 40 °C. D) Microscope images of PU-1.5k$^{0.6}$ gels at increasing temperatures.

sample number (performed in triplicate) limit the accuracy of the swelling degree determinations in contrast to the turbidity measurements. Nonetheless, in comparison to the formerly mentioned studies on similar PU hydrogels, it can be observed that the volume switches between 5 and 40 °C of the pEG-2.0k- ((320 ± 7)%) and pEG-1.5k- ((350 ± 12)%) based hydrogels significantly exceed those reported by Li et al. (pEG-2.0k, ≈100%)[23] and Frydrych et al. (pEG-1.5k, ≈200%).[17] This is likely caused by the additionally incorporation of the hydrophobic DMMI-groups and generally depends on the overall amphiphilic balance. As exemplarily shown for PU-1.5k$^{0.6}$, the temperature-induced deswelling is also accompanied by a significant size reduction corresponding to 83% (25 °C), 69% (45 °C), and finally 63% (55 °C) of the initial diameter at 5 °C (Figure 3D).

2.4. Bio-Linker Attachment and Cell Adhesion

To generate bio-adhesive hydrogel surfaces, we further investigated the possibility to incorporate integrins such as catechol groups or RGD sequences into the PU networks, since both groups are known to promote cell adhesion. To keep the polymer design simple, the initially incorporated DMMI side-groups are also used for the attachment of these bio-linkers. For this purpose, 3,4-(dihydroxyphenyl)propionic acid 16 is coupled with a DMMI functionalized triethylene glycol linker **12** in an HATU mediated amidation to obtain the DMMI-functionalized catechol **6** (**Figure 4**A and Scheme S2, Supporting Information). Analogously, the RGD-alkyne derivate **23** synthesized by solid phase peptide synthesis is coupled with a triethylene glycol-DMMI azide linker **22** in a copper catalyzed azide-alkyne cycloaddition (Figure 4A and Scheme S3, Supporting Information). The triethylene glycol linker ensures the water solubility of both bio-linkers. The schematic incorporation of RGD-DMMI units in the PU gel is shown in Scheme S5, Supporting Information. To further ensure the mechanical integrity of the hydrogels and to allow good material handling in the cell adhesion test, we changed the polymer concentration from 100 to 200 g•L^{-1}.

Analytical evidence of the bio-linker incorporation into the PU gels is provided by ^{1}H magic angle spinning (MAS) NMR spectroscopy (Figure 4B). The ^{1}H MAS NMR spectra of thoroughly dialyzed PU-2.0k (200 g•L^{-1}) gels with 0 mol% RGD

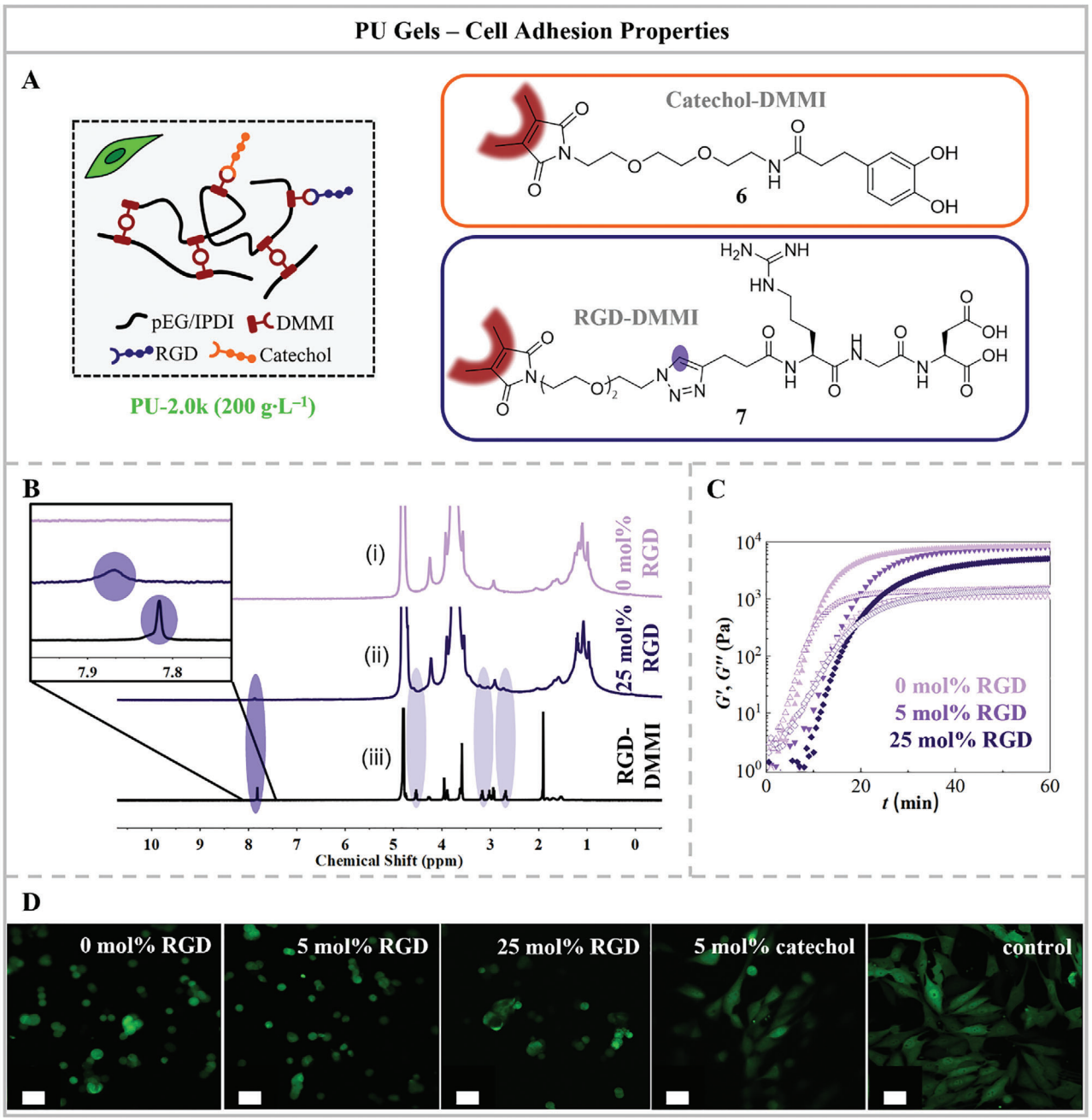

Figure 4. A) Scheme for the incorporation of RGD-DMMI (highlighted in purple) or catechol-DMMI (highlighted in orange) groups into the PU networks to increase their cell adhesive properties. B) ^{1}H MAS NMR spectra of PU-2.0k gels (200 g•L^{-1}) containing 0 mol% (i) and 25 mol% RGD-DMMI (ii) in D_2O and ^{1}H solution NMR spectrum of DMMI-RGD (iii) in D_2O. C) Mechanical strength of PU-2.0k gels (200 g•L^{-1}) with 0, 5, and 25 mol% RGD-DMMI bio-linker. D) CLSM imaging of green-fluorescent cells (MG-63-GFP) after 24 h incubation (37 °C and 5% CO_2) on PU-2.0k gels (200 g•L^{-1}) with 0, 5, and 25 mol% RGD, and 5 mol% catechol. For comparison, a control experiment with cells growing on polystyrene-based petri dishes with cell adhesive properties is also shown. The scale bars refer to 50 µm.

(i) and 25 mol% RGD (ii)(compared to the PU-DMMI groups) are analyzed and compared to the ^{1}H solution NMR spectrum of pure RGD-DMMI **7** (iii). As shown in Figure 4B (ii) the ^{1}H MAS NMR spectrum is dominated by the PU backbone resonances, but the additionally occurring signals at 7.87 ppm (triazole-CH), 4.58 ppm (triazoleN-CH_2), 3.22 ppm (arginine NHC*H*), 3.06 ppm (triazoleC-CH_2CH$_2$), and 2.73 ppm (triazoleC-CH$_2$CH_2) can be assigned to the RGD-DMMI and indicate the successful incorporation into the network. An especially clearly visible example is the resonance of the triazole proton at $\delta = 7.82$ ppm. The weak, low field-shoulder observed in the reference spectrum in aqueous solution is presumably caused by a second tautomeric form

of the triazole.[28,29] Nonetheless, it can be noted that the signal of the RGD-DMMI linker is shifted to $\delta = 7.87$ ppm inside the gel and significantly broadened as shown by the increased full width at half height fwhh (solution: fwhh = 2.42 Hz; gel: fwhh = 9.05 Hz). A similar broadening is observed for all related signals and can be explained by the confinement in the gel pores resulting in reduced chain dynamics. An analogous measurement with 5 mol% RGD showing the same characteristic signals with lower intensities is provided in the Figure S4, Supporting Information.

Since the DMMI groups that react with a linker molecule cannot contribute to the 3D crosslinking reaction, it is further investigated how the attachment of RGD sequences influences the gelation of the PU-2.0k gels (200 g•L^{-1}). As shown in Figure 4C, the addition of 5 mol% RGD to the precursor solution does not significantly affect the plateau modulus. If the concentration is however increased to 25 mol%, a 40% lower plateau modulus results. In addition to this investigation during the gelation process, it is also probed how the incorporation of the catechol linker influences the mechanical properties of the purified gels under equilibrium swelling conditions (Figure S5, Supporting Information). The results coincide with the former findings and demonstrate that the applicable concentration range of the bio-linkers is limited by the accessible number of DMMI groups in the PU chains.

To analyze the cell adhesive properties of PU gels with RGD or catechol bio-linkers, cell experiments are performed (Figure 4D). For this purpose, green-fluorescent osteoblasts (MG-63-GFP) are cultured on PU-2k gels (200 g•L^{-1}) with 0 and 5 mol% RGD and catechol. After 24 h, the gels are analyzed by Confocal Laser Scanning Microscopy (CLSM). The cells on the 0 and 5 mol% RGD gels show a spherical morphology, indicating a low cell adhesion capacity. By contrast, the cells on the 5 mol% catechol gels show an elongated morphology comparable to the control experiment, indicating a pronounced cell adhesion. Consequently, the question arises as to why the cells adhere to the catechol-based but not to the RGD-based PU-2k hydrogels. This is likely due to the insufficient amount of integrins in the RGD-based polymer, as the cells require a certain concentration of integrins to adhere.[30,31] Although the same concentration of RGD and catechol units was used, the total integrin density in catechol is higher because serum proteins from the culture medium adhere to the catechol units, which have a higher number of integrin binding sites than single amino acid sequences such as RGD.[32,33] To probe whether an analogous behavior can be achieved at a higher RGD concentration, the experiment is repeated with a 25 mol% RGD containing gel. However, as can be seen in Figure 4D, this increase in concentration is still insufficient, which can be explained by the decreasing mechanical gel strength. The more RGD sequences are incorporated into the network, the fewer network junctions can be formed which increases the swelling degree of the corresponding hydrogels. Due to this counteracting behavior, an increase of the RGD concentration does not efficiently increase the RGD density in the network and thus prevents an improvement of the cell attachment. Beyond that, sufficiently stable gels are not obtained above 25 mol% RGD. Hence, it is not practicable to improve the cell adhesion by a further increase of the RGD concentration. Based on this comparison, the catechol linkers are found to be a suitable way to increase the biocompatibility of the PU hydrogels.

3. Conclusion

In this study, thermoresponsive, pEG-IPDI based PUs with dimerizable DMMI side groups are synthesized. The cloud point temperatures of the dilute, aqueous PU solutions depend linearly on the molar ratio between hydrophilic EG and hydrophobic IPDI and DMMI groups and can be varied from 5 to over 90 °C. Soft hydrogels are obtained through the UV-light induced crosslinking of the precursor polymers in the presence of a photosensitizer. The equilibrium swelling ratio ($Q_{5\,°C}$ = 2700–7800%) and gel strength in terms of the plateau modulus (G' = 200–4000 Pa) are both determined by the precursor polymer concentration and the average DMMI density. The swelling ratio switches of the hydrogels ($Q_{5\,°C}/Q_{40\,°C}$) reflect the cloud point temperature dependency on the amphiphilic balance and increase from 180% to 350% for the more hydrophobic PU compositions. Furthermore, the cell adhesive properties of these PU gels can be significantly improved by incorporating low concentrations of a catechol bio-linker through DMMI side groups without significantly affecting the mechanical properties.

Supporting Information

Supporting Information is available from the Wiley Online Library or from the author.

Acknowledgements

K.B. and E.S. contributed equally to this work. Parts of the results of this study were acquired with a Confocal Laser Scanning Microscope funded in part by the Major Research Instrumentation Program of the German Research Foundation under grant No. INST 247/878-1 FUGG. The authors wish to thank Ronald E. Unger (JGU Mainz, Institute for Pathology) for providing osteoblasts expressing GFP (MG-63-GFP).

Open access funding enabled and organized by Projekt DEAL.

Conflict of Interest

The authors declare no conflict of interest.

Data Availability Statement

The data that support the findings of this study are available from the corresponding author upon reasonable request.

Keywords

cell adhesion, soft biomaterials, thermoresponsive polyurethane hydrogels, UV crosslinking

Received: August 3, 2021
Revised: September 17, 2021
Published online: October 21, 2021

[1] F. Doberenz, K. Zeng, C. Willems, K. Zhang, T. Groth, *J. Mater. Chem. B* **2020**, *8*, 607.

[2] L. Klouda, A. G. Mikos, *Eur. J. Pharm. Biopharm.* **2008**, *68*, 34.
[3] H. Fan, J. P. Gong, *Macromolecules* **2020**, *53*, 2769.
[4] C. A. Deforest, K. S. Anseth, *Annu. Rev. Chem. Biomol. Eng.* **2012**, *3*, 421.
[5] J. J. Rice, M. M. Martino, L. De Laporte, F. Tortelli, P. S. Briquez, J. A. Hubbell, *Adv. Healthcare Mater.* **2013**, *2*, 57.
[6] D. Dippold, A. Cai, M. Hardt, A. R. Boccaccini, R. E. Horch, J. P. Beier, D. W. Schubert, *Mater. Sci. Eng., C* **2019**, *95*, 217.
[7] Y. Zhang, J. Hu, X. Zhao, R. Xie, T. Qin, F. Ji, *ACS Appl. Bio Mater.* **2019**, *2*, 1056.
[8] K. Wei, X. Chen, P. Zhao, Q. Feng, B. Yang, R. Li, Z. - Y. Zhang, L. Bian, *ACS Appl. Mater. Interfaces* **2019**, *11*, 16328.
[9] T. J. Dennes, J. Schwartz, *Soft Matter* **2008**, *4*, 86.
[10] E. Stengelin, B. Nzigou Mombo, M. Mondeshki, G. L. Beltramo, M. A. Lange, P. Schmidt, H. Frerichs, S. V. Wegner, S. Seiffert, *Macromol. Biosci.* **2021**, *21*, 2100209.
[11] A. Bin Imran, K. Esaki, H. Gotoh, T. Seki, K. Ito, Y. Sakai, Y. Takeoka, *Nat. Commun.* **2014**, *5*, 5124.
[12] V. Pertici, C. Pin-Barre, C. Rivera, C. Pellegrino, J. Laurin, D. Gigmes, T. Trimaille, *Biomacromolecules* **2019**, *20*, 149.
[13] H. Sardon, J. P. K. Tan, J. M. W. Chan, D. Mantione, D. Mecerreyes, J. L. Hedrick, Y. I. Y. Yang, *Macromol. Rapid Commun.* **2015**, *36*, 1761.
[14] L. Polo Fonseca, R. B. Trinca, M. I. Felisberti, *Int. J. Pharm.* **2018**, *546*, 106.
[15] M. Ding, N. Song, X. He, J. Li, L. Zhou, H. Tan, Q. Fu, Q. Gu, *ACS Nano* **2013**, *7*, 1918.
[16] F. Oveissi, S. Naficy, A. Lee, D. S. Winlaw, F. Dehghani, *Mater. Today Bio* **2020**, *5*, 100038.
[17] M. Frydrych, S. Román, N. H. Green, S. Macneil, B. Chen, *Polym. Chem.* **2015**, *6*, 7974.
[18] H. Fu, H. Gao, G. Wu, Y. Wang, Y. Fan, J. Ma, *Soft Matter* **2011**, *7*, 3546.
[19] J. P. Santerre, K. Woodhouse, G. Laroche, R. S. Labow, *Biomaterials* **2005**, *26*, 7457.
[20] L. I. Ronco, A. Basterretxea, D. Mantione, R. H. Aguirresarobe, R. J. Minari, L. M. Gugliotta, D. Mecerreyes, H. Sardon, *Polymer* **2017**, *122*, 117.
[21] D. Aoki, H. Ajiro, *Macromol. Rapid Commun.* **2018**, *39*, 1800239.
[22] D. Aoki, H. Ajiro, *Macromol. Rapid Commun.* **2021**, *42*, 2100128.
[23] K. Li, C. Zhou, S. Liu, F. Yao, G. Fu, L. Xu, *React. Funct. Polym.* **2017**, *117*, 81.
[24] S. Seiffert, W. Oppermann, K. Saalwächter, *Polymer* **2007**, *48*, 5599.
[25] S. V. Karpov, V. P. Lodygina, V. V. Komratova, A. S. Dzhalmukhanova, G. V. Malkov, E. R. Badamshina, *Kinet. Catal.* **2016**, *57*, 422.
[26] H.-K. Ono, F. N. Jones, S. P. Pappas, *J. Polym. Sci., Part B: Polym. Lett. Ed.* **1985**, *23*, 509.
[27] K. Breul, S. Seiffert, *Polym. Chem.* **2021**, *12*, 2305.
[28] L. Lunazzi, F. Parisi, D. Macciantelli, *J. Chem. Soc., Perkin Trans. 2* **1984**, 1025.
[29] J. R. Cox, S. Woodcock, I. H. Hillier, M. A. Vincent, *J. Phys. Chem.* **1990**, *94*, 5499.
[30] J. A. Rowley, D. J. Mooney, *J. Biomed. Mater. Res.* **2002**, *60*, 217.
[31] J. A. Burdick, K. S. Anseth, *Biomaterials* **2002**, *23*, 4315.
[32] S. Spaans, P. P. K. H. Fransen, B. D. Ippel, D. F. A. De Bont, H. M. Keizer, N. A. M. Bax, C. V. C. Bouten, P. Y. W. Dankers, *Biomater. Sci.* **2017**, *5*, 1541.
[33] W.-B. Tsai, W.-T. Chen, H.-W. Chien, W.-H. Kuo, M.-J. Wang, *Acta Biomater.* **2011**, *7*, 4187.

